Original Article | Cardiovascular Imaging

eISSN 2005-8330
https://doi.org/10.3348/kjr.2020.0249
Korean J Radiol 2021;22(1):97-105

Korean Journal of Radiology
KJR

Dynamic CT Myocardial Perfusion Imaging in Patients without Obstructive Coronary Artery Disease: Quantification of Myocardial Blood Flow according to Varied Heart Rate Increments after Stress

Lihua Yu, MD[1]*, Xiaofeng Tao, MD[2]*, Xu Dai, MD[1], Ting Liu, MD[3], Jiayin Zhang, MD[1]

[1]Institute of Diagnostic and Interventional Radiology, Shanghai Jiao Tong University Affiliated Sixth People's Hospital, Shanghai, China; [2]Department of Radiology, Shanghai Ninth People's Hospital, Shanghai Jiao Tong University School of Medicine, Shanghai, China; [3]Department of Radiology, First Affiliated Hospital of China Medical University, Shenyang, China

Objective: The present study aimed to investigate the association between myocardial blood flow (MBF) quantified by dynamic CT myocardial perfusion imaging (CT-MPI) and the increments in heart rate (HR) after stress in patients without obstructive coronary artery disease.

Materials and Methods: We retrospectively included 204 subjects who underwent both dynamic CT-MPI and coronary CT angiography (CCTA). Patients with more than minimal coronary stenosis (diameter ≥ 25%), history of myocardial infarction/revascularization, cardiomyopathy, and microvascular dysfunction were excluded. Global MBF at stress was measured using hybrid deconvolution and maximum slope model. Furthermore, the HR increments after stress were recorded.

Results: The median radiation dose of dynamic CT-MPI plus CCTA was 5.5 (4.5–6.8) mSv. The median global MBF of all subjects was 156.4 (139.8–180.4) mL/100 mL/min. In subjects with HR increment between 10 to 19 beats per minute (bpm), the global MBF was significantly lower than that of subjects with increment between 20 to 29 bpm (153.3 mL/100 mL/min vs. 171.3 mL/100 mL/min, $p = 0.027$). This difference became insignificant when the HR increment further increased to ≥ 30 bpm.

Conclusion: The global MBF value was associated with the extent of increase in HR after stress. Significantly higher global MBF was seen in subjects with HR increment of ≥ 20 bpm.

Keywords: *Coronary artery disease; Computed tomography; Angiography; Myocardial perfusion imaging; Myocardial blood flow*

INTRODUCTION

Dynamic CT myocardial perfusion imaging (CT-MPI) combined with coronary CT angiography (CCTA) is a "one-stop shop" imaging modality, which provides anatomical and functional information of the coronary arteries. Compared to static CT-MPI, dynamic CT-MPI enables quantification of different perfusion parameters, such as myocardial blood flow (MBF) and myocardial blood volume, for more precise evaluation of myocardial ischemia (1-

Received: December 13, 2019 **Revised:** May 5, 2020 **Accepted:** May 9, 2020
This study is supported by National Natural Science Foundation of China (Grant No.: 81671678, 81871435), Medical Guidance Scientific Research Support Project of Shanghai Science and Technology Commission (Grant No.: 19411965100), Shanghai Municipal Education Commission-Gaofeng Clinical Medicine Grant Support (Grant No.: 20161428) and Innovative research team of high-level local universities in Shanghai.

*These authors contributed equally to this work.

Corresponding author: Jiayin Zhang, MD, Institute of Diagnostic and Interventional Radiology, Shanghai Jiao Tong University Affiliated Sixth People's Hospital, No.600, Yishan Rd, Shanghai 200233, China.
• E-mail: andrewssmu@msn.com

4). With the recent introduction of third generation dual source CT (DSCT), it is now technically feasible to perform dynamic CT-MPI at lower radiation doses compared to previous CT scanners (5-8).

Although MBF is considered the best parameter for diagnosing myocardial ischemia, the ranges of MBF in normal, non-ischemic, and ischemic myocardial segments varied between studies using different CT scanners and calculation algorithms (1-4, 9). In addition, the response to adenosine has an impact on the extent of hyperemic status, which could be reflected by an increase in heart rate (HR) after stress (10). Thus, it is of clinical importance to identify the association between the extent of stress-related increase in HR and the absolute MBF, and the possible relation of an increase in HR with adequate stress response, as reflected by hyperemic MBF. Therefore, we aimed to investigate the association between MBF quantified by dynamic CT-MPI and HR increments after stress in patients without obstructive coronary artery disease (CAD).

MATERIALS AND METHODS

Patient Population

The Ethics Committee of the hospital approved this retrospective study and the need for informed consent from patients was waived. We retrospectively searched the database of a tertiary hospital between October 2016 and June 2019 to screen all patients who had undergone dynamic CT-MPI plus CCTA. The clinical indication for CT-MPI plus CCTA was to diagnose myocardial ischemia in symptomatic patients with intermediate to high pre-test probability of obstructive CAD. Inclusion criterion was dynamic CT-MPI plus CCTA that revealed normal coronary artery or with minimal coronary stenosis (defined as diameter of stenosis (DS) < 25% in any epicardial vessel). Exclusion criteria were as follows: 1) patients with history of myocardial infarction; 2) patients with concomitant cardiomyopathies or structural heart disease; 3) patients with history of revascularization; 4) patients with clinical diagnosis of microvascular dysfunction according to the index of microvascular resistance; and 5) patients with impaired image quality of dynamic CT-MPI or CCTA (Fig. 1).

A total of 285 patients with dynamic CT-MPI plus CCTA were retrospectively reviewed. Eighty-one patients were excluded due to various reasons (details shown in Fig. 1). Finally, a total of 204 patients (mean age, 65.3 ± 12.2 years; range, 28 to 90 years; 143 men [mean age 64.8 ± 12.3 years, range 28 to 90 years] and 61 women [mean age,

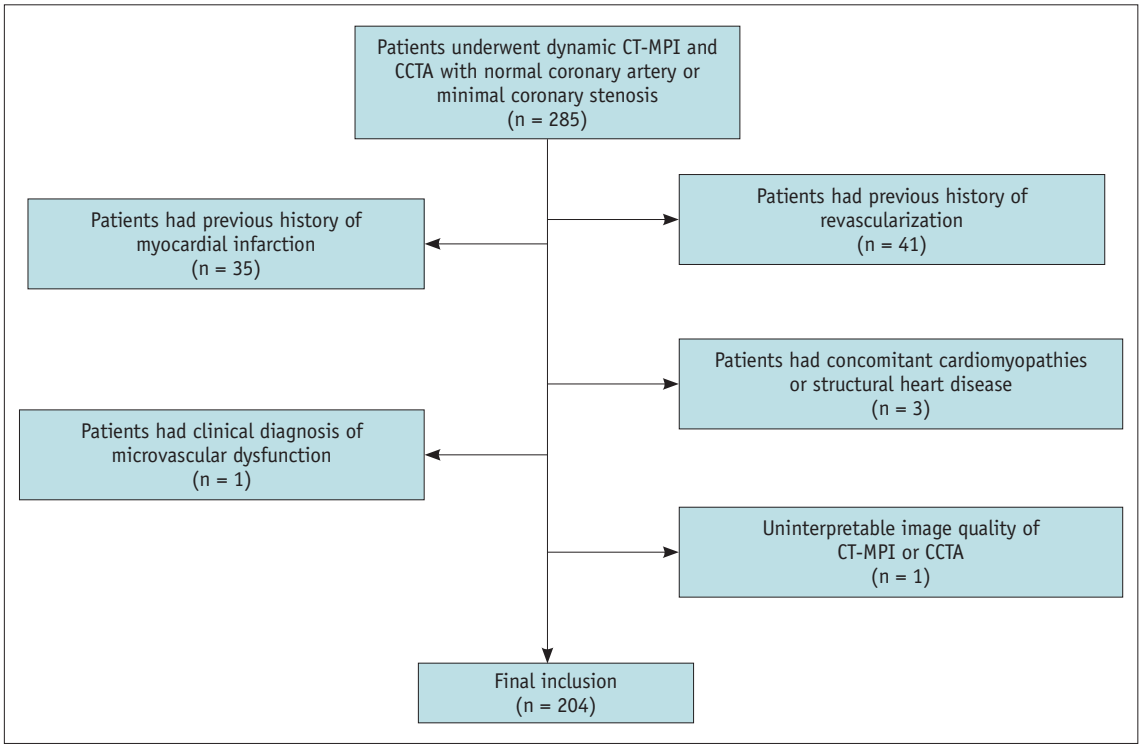

Fig. 1. Flow chart of inclusion and exclusion criteria. CCTA = coronary CT angiography, CT = computed tomography, MPI = myocardial perfusion imaging

https://doi.org/10.3348/kjr.2020.0249

Korean Journal of Radiology
KJR

66.6 ± 12.1 years; range, 30 to 85 years], p = 0.345) were included in the analysis.

Dynamic CT-MPI and CCTA Protocol

In all patients, a comprehensive imaging protocol integrating the calcium score, dynamic stress CT-MPI, and CCTA was used. All patients were instructed to refrain from caffeine intake 24 hours prior to the examination and from the use of beta-blockers and theophylline on the examination day. Dynamic CT-MPI was performed using third generation DSCT (SOMATOM Force, Siemens Healthineers). Calcium score was calculated to measure the calcification burden of each pericardial vessel. The scan range of dynamic CT-MPI was determined based on the calcium score images to cover the left ventricle (LV) completely as well as all coronary arteries. Adenosine triphosphate (ATP) was intravenously infused over 3 minutes at 160 μg/kg/min before triggering the MPI acquisition. A fixed volume of contrast media (50 mL, iopromide, 370 mg iodine/mL, Bayer AG) was given in a bolus injection at the rate of 6 mL/s in all patients, followed by a 40 mL saline flush using a dual-barrel power injector (Tyco). Dynamic CT-MPI acquisition was started 4 seconds after the onset of contrast injection. The end-systolic phase (triggered at 250 ms after the R wave in all patients) was set for dynamic acquisition using a shuttle mode technique with coverage of 10.5 cm for complete imaging of the LV. Scans were launched every second or third heart cycle according to patient's HR, resulting in a series of 10 to 15 phases acquired over a fixed period of 32 seconds. The acquisition parameters of dynamic CT-MPI were as follows: collimation was 96 x 0.6 mm, CARE kV (Siemens Healthineers) was used and the reference tube voltage was 80 kVp; rotation time was 250 ms, CARE Dose 4D (Siemens Healthineers) was used and the effective current was 300 mAs; reconstructed slice thickness was 3 mm and reconstructed slice interval was 2 mm. Baseline HR was measured before the start of ATP infusion, whereas peak HR was recorded as maximal HR 3 minutes after infusion of ATP. HR increment was defined as the difference between maximal and baseline HRs.

Nitroglycerin was given sublingually in all patients 5 minutes after dynamic CT-MPI, prior to the acquisition of CCTA. Prospective electrocardiogram (ECG)-triggered sequential acquisition was performed in all patients for CCTA using a bolus tracking technique, with regions of interest placed in the ascending aorta. A bolus of contrast media was injected into the antecubital vein at the rate of 4–5 mL/s, followed by a 40 mL saline flush using the dual-barrel power injector. The amount of the contrast media was determined according to the patient's body weight (Table 1). Prospective ECG-triggered sequential acquisition was performed in all patients for CCTA, with the triggering window set to cover from end-systolic to mid-diastolic phase (35% to 75% of R-R interval), with collimation = 96 x 0.6 mm, reconstructed slice thickness = 0.75 mm, reconstructed slice interval = 0.5 mm, rotation time = 250 ms, and application of automated tube voltage and current modulation (CARE kV and CARE Dose 4D). The reference tube current was set as 320 mAs and the reference tube voltage was set as 100 kVp.

CCTA-Based Stenosis Analysis

Axial images were reconstructed with the smooth kernel (Bv 40) using the third generation iterative reconstruction technique (strength 3, ADMIRE, Siemens Healthineers). Data were transferred to an offline workstation (syngo.via, Siemens Healthineers) and the dataset of best phase was used for further analyses.

The DS was defined as (reference diameter - minimal lumen diameter) / reference diameter. Only patients with normal coronary artery or minimal coronary stenosis (defined as DS < 25% at any epicardial vessel) were included for the further evaluation of normal MBF range.

CT-MPI Analysis

The CT-MPI data was reconstructed using a dedicated

Table 1. Protocol of Contrast Medium Delivery and Dose Saving Technique of Dynamic CT-MPI and CCTA

Scan	Scan Mode	BMI	CM Volume (mL)	Injection Rate (mL/s)	CARE kV	Reference Voltage (kV)	CARE Dose 4D	Reference Current (mAs)
Dynamic CT-MPI	Shuttle mode	Any	50	6.0	On	80	On	300
CCTA	Prospective ECG-triggered sequential acquisition	< 18.0	40	4.0	On	100	On	320
		18.0–23.9	50	4.5	On	100	On	320
		≥ 24.0	60	5.0	On	100	On	320

CARE kV and CARE Dose 4D, Siemens Healthineers. BMI = body mass index, CCTA = coronary CT angiography, CM = contrast medium, CT = computed tomography, ECG = electrocardiogram, MPI = myocardial perfusion imaging

https://doi.org/10.3348/kjr.2020.0249

kernel for reduction of iodine beam-hardening artifacts (Qr36) and analyzed using a CT-MPI software package (Myocardial perfusion analysis: VPCT, Siemens Healthineers). Motion correction was applied in necessary cases to correct for breathing-related mis-registration of the LV. For quantification of MBF, the influx of contrast medium was measured using the arterial input function (AIF). The AIF was sampled in the descending aorta by including both the cranial and caudal sections. For quantification of the MBF and other parameters, the myocardial time attenuation curves were coupled with the AIF using a hybrid deconvolution and maximum slope model (11, 12).

Image noise of dynamic perfusion data was measured in the LV cavity on axial images using a region of interest (ROI) of 1 cm^2. Image noise was defined as the standard deviation (SD) of the pixel values within the ROI in the first phase of dynamic dataset before arrival of the contrast medium in the LV (12). Similarly, maximal enhancement was measured as the mean HU value within the LV cavity of the same ROI in the phase of peak enhancement (13).

For quantification of MBF, the ROI was manually placed in the sample MBF on a segment base based on the 17-segment model (14). The ROI was drawn to cover the whole segment with exclusion of endocardial and epicardial interfaces. The short-axis view of the myocardial color-coded map was used for quantification of all segments except the apical segment, which was evaluated on the vertical long-axis view. MBF of all measured segments were individually recorded as $MBF_{segment}$ whereas the patient-based global MBF was automatically measured by the VPCT software using previously reported methods (15).

Two cardiovascular radiologists (with 12 years and 4 years of experience in cardiovascular imaging, respectively) independently evaluated all segments with knowledge of CCTA results. The mean values of measurements between the two observers were used to determine the normal range of MBF.

Statistical Analyses

Statistical analyses were performed using SPSS Statistics 22.0 (IBM Corp.). One-sample Kolmogorov-Smirnov test was first used to check the assumption of normal distribution. Quantitative variables with normal distribution were expressed as mean ± SD, while median and interquartile range (IQR) was used for variables that were not normally distributed. *T* test was used to examine the age differences between sexes. Kruskal-Wallis test was used for multiple comparisons among global MBF of different HR increment subgroups after stress and among $MBF_{segment}$ of different segments. A Dunn-Bonferroni test for post hoc comparisons was used to identify differences between pairs of groups. Mann-Whitney U test was used for comparison between global MBF of subgroups with different scan intervals. Intra-observer and inter-observer agreements of MBF measurement were tested by intraclass correlation coefficients (ICCs). A two-tailed probability value of $p < 0.05$ was considered statistically significant.

RESULTS

Characteristics of the Study Population

Detailed demographic data of included patients are presented in Table 2.

Image Quality and Radiation Dose of Dynamic CT-MPI

The median dose length product of dynamic CT-MPI plus CCTA and calcium score was 390.9 mGy x cm (IQR, 318.0–487.0 mGy x cm, range 202.0 to 965.0 mGy x cm) and 28.0

Table 2. Demographic Data

Characteristics	
Patient number	204
Age (years)	65.3 ± 12.2
Sex	
Females	61 (29.9)
Males	143 (70.1)
Weight (kg)	67.2 (IQR, 60.0–73.4)
BMI	24.0 (IQR, 22.5–26.0)
Risk factors	
Hypertension	134 (65.7)
Hyperlipidemia	82 (40.2)
Smoking	73 (35.8)
Diabetes	62 (30.4)
Pretest probability*	
15–85	194 (95.1)
> 85	10 (4.9)
CAD-RADS classification	
0	13 (6.4)
1	191 (93.6)
Agatston calcium score	35.5 (IQR, 0–230.1)
HR (beats/min)	
Baseline	69.5 (IQR, 63.0–78.8)
After stress	88.0 (IQR, 78.0–98.0)

Values are mean ± standard deviation, n (%), or median (IQR). *Calculated by using the updated Diamond and Forrester Chest Pain Prediction Rule. CAD = coronary artery disease, HR = heart rate, IQR = interquartile range

https://doi.org/10.3348/kjr.2020.0249

Korean Journal of Radiology
KJR

mGy x cm (IQR, 24.0–33.6 mGy x cm, range 15.2 to 56.6 mGy x cm), respectively, corresponding to 5.5 mSv (IQR, 4.5–6.8 mSv, range 2.8 to 13.5 mSv) and 0.4 mSv (IQR, 0.3–0.5 mSv, range 0.2 to 0.8 mSv) when using 0.014 as the conversion factor (16). The mean image noise measured in the first phase of dynamic dataset before arrival of the contrast medium in the LV was 23.9 ± 3.6 HU. The maximal enhancement of the LV cavity was 748.9 ± 144.8 HU.

Relationship between MBF and HR Increments after Stress

The ICC of intra-observer agreement for observer 1, observer 2, and inter-observer measurement for MBF were 0.926 (95% confidence interval [CI] = 0.866–0.960, p < 0.001), 0.919 (95% CI = 0.841–0.958, p < 0.001), and 0.910 (95% CI = 0.841–0.948, p < 0.001), respectively.

Table 3. Absolute Global MBF of Groups with Different HR Increment

HR Range	Global MBF (mL/100 mL/min)
Overall (n = 204)	156.4 (IQR, 139.8–180.4) (range, 104.8–245.9)
HR increment (beats/min)	
0–9 (n = 34)	141.6 ± 24.4 (range, 104.8–198.1)
10–19 (n = 92)	153.3 (IQR, 137.6-174.6) (range, 109.2–215.3)
20–29 (n = 59)	171.3 ± 31.8 (range, 114.1–271.7)
≥ 30 (n = 19)	183.0 ± 35.3 (range, 136.8–245.9)

Values are mean ± SD or median (IQR). MBF = myocardial blood flow

According to the current findings, the median global MBF of all patients was 156.4 (IQR, 139.8–180.4) mL/100 mL/min. However, different ranges of absolute MBF were revealed in accordance with different HR increments after stress. The lowest MBF was found in the subgroup with minimal increase in HR, whereas the highest MBF was observed in the subgroup with maximal increase in HR (Table 3, Figs. 2–4). For subjects with HR increment between 10 to 19 beats per minute (bpm), the global MBF was significantly lower than that of subjects with HR increment between 20 to 29 bpm (153.3 mL/100 mL/min vs. 171.3 mL/100 mL/min, p = 0.027). However, this difference became insignificant when HR increment further increased to ≥ 30 bpm. In addition, in the segment-based analysis, value of the basal inferoseptal $MBF_{segment}$ was significantly lower than that of all other segments (all p < 0.01). However, no difference was observed between any other segments (Fig. 5). There was no significant difference in global MBF between subgroups with CT-MPI scan interval of one and two heart cycles (156.1 [IQR, 138.0–176.8] mL/100 mL/min vs. 157.0 [IQR, 141.8–199.8] mL/100 mL/min, p = 0.218).

DISCUSSION

The current study revealed that the global MBF value was associated with the extent of change in HR after stress. Significantly higher global MBF was seen in subjects with HR increment of ≥ 20 bpm.

One of the major benefits of dynamic CT-MPI lies in its absolute quantification of MBF for precise evaluation of myocardial ischemia (1-4). However, it must be noted that the best cut-off value for differentiating ischemic and non-

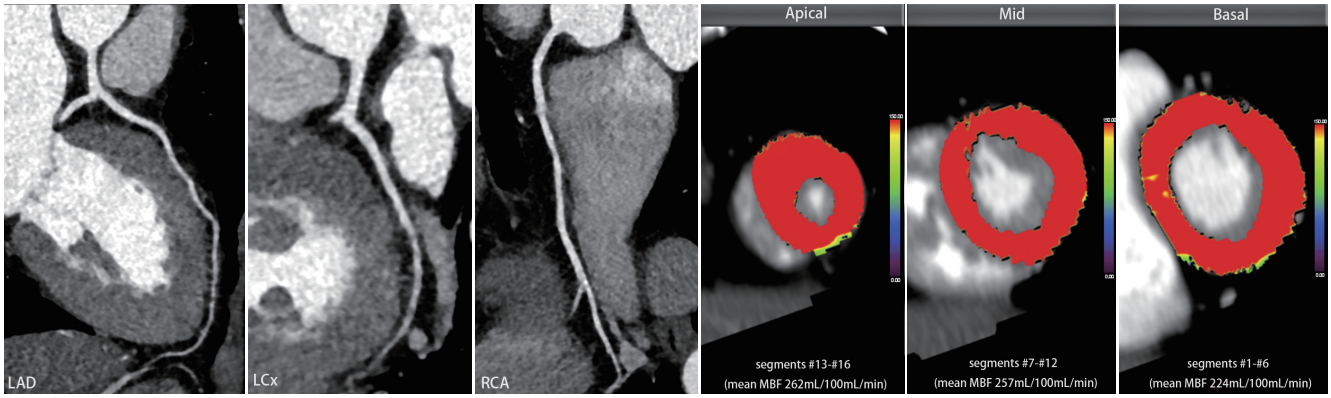

Fig. 2. Representative case of high-quantified MBF derived from a subject with maximal increase in HR after stress (HR increased by 24 beats/min). CPR image shows normal coronary arteries without atherosclerosis or stenosis. Short-axis views of CT-MPI from the apical to basal segments reveal high MBF values from 224 mL/100 mL/min to 262 mL/100 mL/min. CPR = curved planar reformation, HR = heart rate, LAD = left anterior descending, LCX = left circumflex, MBF = myocardial blood flow, RCA = right coronary artery

https://doi.org/10.3348/kjr.2020.0249

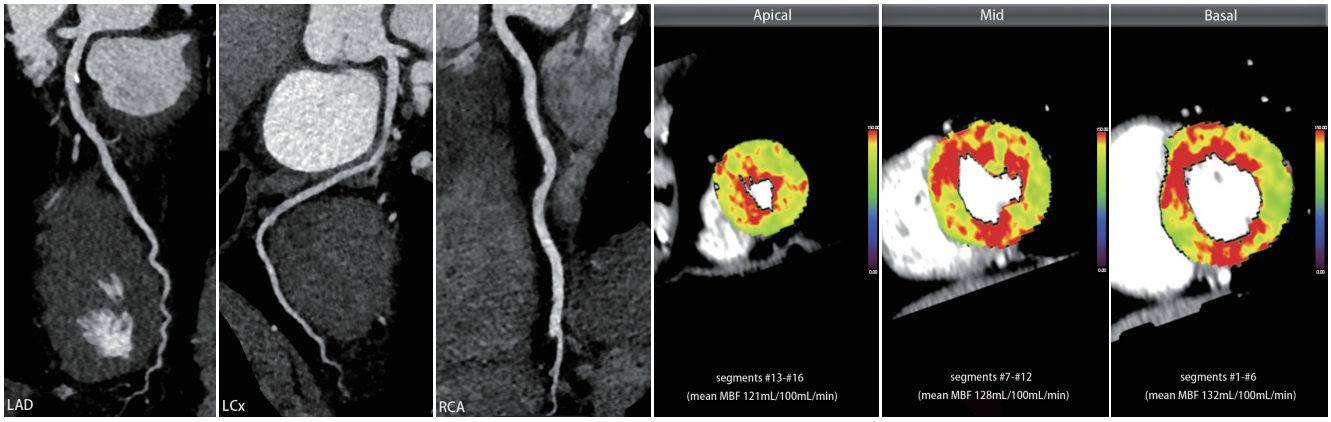

Fig. 3. Representative case of low-quantified MBF derived from a subject with minimal increase in HR after stress (HR increased by 9 beats/min). CPR image shows coronary arteries with atherosclerosis and minimal stenosis (< 25%) at the proximal LAD and middle RCA. Short-axis views of CT-MPI from the apical to basal segments reveal low MBF values from 121 mL/100 mL/min to 132 mL/100 mL/min.

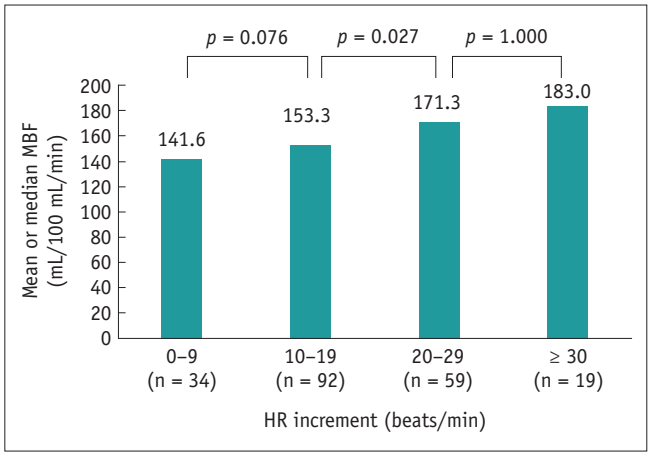

Fig. 4. Global MBF values of subgroups with different HR increments after stress. The lowest MBF was found in the subgroup with minimal increase in HR, whereas the highest MBF was observed in the subgroup with maximal increase in HR.

ischemic lesions varied between different studies, from 75 mL/100 mL/min to 103 mL/100 mL/min (1-4, 9, 17-19). Moreover, studies have reported different values of the mean MBF in normal subjects (20, 21). This discrepancy in the absolute MBF could be potentially explained by the different calculation algorithms applied. According to a recent *in vivo* animal study, the absolute MBF values varied significantly between different calculation models (22). Therefore, exploration of the normal range of absolute MBF based on specific calculation algorithms is of clinical importance to guide image interpretation of dynamic CT-MPI.

The current study revealed that the median absolute stress MBF was 156.4 mL/100 mL/min (IQR, 139.8 mL/100 mL/min–180.4 mL/100 mL/min), as quantified by the hybrid deconvolution and maximum slope model on the platform of third generation DSCT. This normal stress MBF value was lower than that derived from positron emission tomography-MPI, which is usually between 300 mL/100 g/min to 500 mL/100 g/min (23). The calculation algorithm used in the present study could explain this discrepancy. The current model (hybrid deconvolution and maximum slope) was designed for the relatively low sampling rate (every 2–3 seconds) of shuttle mode acquisition. Despite its robust clinical value in detecting myocardial ischemia (4), the model is associated with the drawback of the maximum slope method for absolute quantification of MBF, which resulted in significantly lower MBF compared to other calculation algorithms (22). Therefore, direct comparison of the absolute MBF value generated from different imaging modalities and calculation algorithms should be avoided in clinical practice. In addition, heterogeneity in the segment-based MBF was observed in the present study as the basal inferoseptal segment demonstrated a significantly lower value compared to other segments. This is in line with a previous CT-MPI study, which reported that MBF of the septal wall might be lower than that of the anterior and lateral walls (123.5 ± 31.0 mL/100 g/min vs. 133.3 ± 29.8 mL/100 g/min and 148.6 ± 32.7 mL/100 g/min, respectively) (20). This could be potentially ascribed to the anatomical feature of the septal wall, wherein the blood supply originates from intramural septal branches rather than from direct branches of the epicardial arteries. As dynamic CT-MPI was acquired during the end-systolic phase, the intramural arteries were maximally compressed by the septal myocardium; therefore, the perfusion pattern of the septal wall might be different from other segments.

Another important finding of the current study was the

https://doi.org/10.3348/kjr.2020.0249

Korean Journal of Radiology
KJR

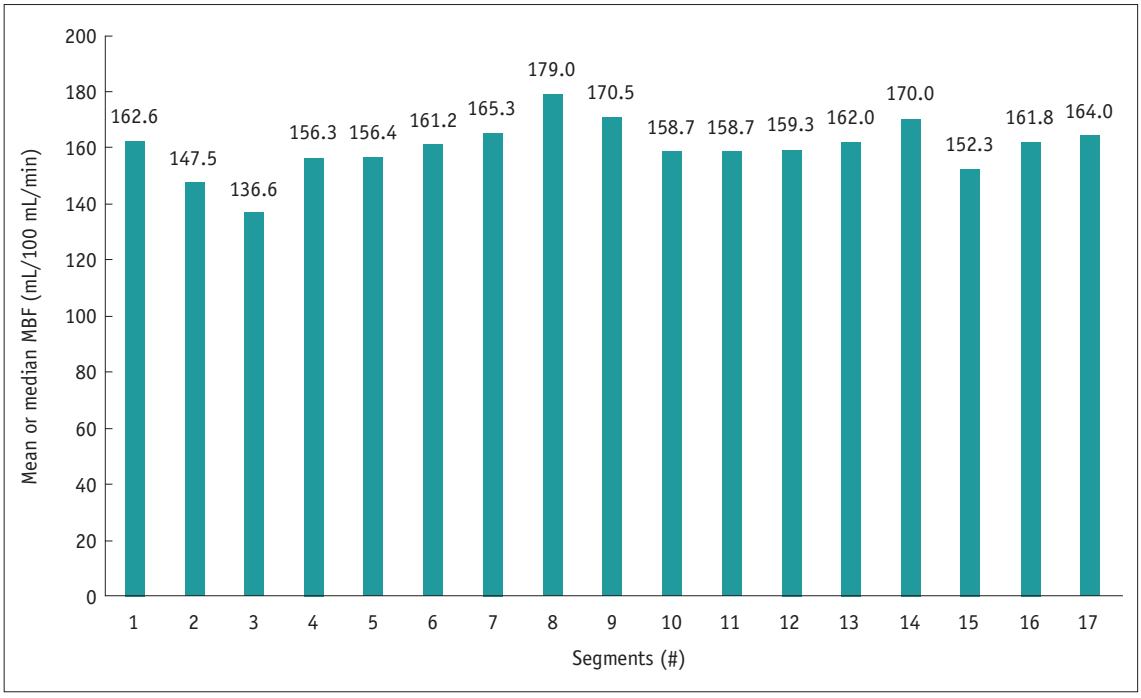

Fig. 5. MBF values of all myocardial segments based on the 17-segment model. Segment #3 (basal inferoseptal) had significantly lower MBF compared to any other segments (all $p < 0.01$). This difference was not significant between all other segments.

variation in MBF based on the change in HR after stress. This could be explained by the variation in individual response to vasodilators and consequently the hyperemic status (maximal or sub-maximal). As revealed by previous MR-MPI studies, maximal hyperemia was not achieved in 18% of the total patients using the standard stress dose of adenosine (10). Similarly, this phenomenon was also observed in the current study using quantitative dynamic CT-MPI. In the present study, significantly higher global MBF was seen in subjects with HR increment of ≥ 20 bpm. This discrepancy could be mainly explained by the suboptimal stress effect in the subgroup with HR increment of < 20 bpm. In addition, subjects with HR increment of ≥ 20 bpm (subgroups 20 to 29 bpm and ≥ 30 bpm) had similar global MBF regardless of the presence of very high HR increment. Therefore, HR increment of ≥ 20 bpm might be a simple indicator of maximal hyperemia.

In light of the above findings, the potential clinical implications of the current study lie in the following two aspects. First, use of a fixed ATP infusion protocol might be inappropriate in terms of achieving maximal hyperemia in all patients. In the current study, we fixed the ATP infusion time at 3 minutes before triggering the CT-MPI acquisition, similar to that reported in a previous study (24). This protocol resulted in a rather heterogeneous distribution of global MBF in different subgroups of HR increments after stress. Maximal hyperemia might not be achieved in a relatively large proportion of the current cohort, especially in subjects with minimal increase in HR after stress. A more flexible infusion protocol, such as extending the duration of infusion in patients with smaller increase in HR, would be favorable to optimize the hyperemic effect. Second, an increase in HR of ≥ 20 bpm might be a simple and useful indicator of maximal hyperemia. In patients with an increase in HR of < 20 bpm at the end of the third minute, intravenous administration of ATP should be prolonged to better achieve maximal hyperemia.

Despite the above findings, the current study has several limitations. First, all patients were scanned with the third generation DSCT, and MBF was calculated by the hybrid deconvolution and maximum slope model. Different calculation algorithms dramatically affect the absolute value of MBF (22); therefore, the present normal range of MBF cannot be applied to the results generated from other algorithms, which limits the generalizability of the current findings. In addition, although only patients with normal coronary artery or minimal coronary stenosis were included in the analysis, they were not completely "normal" subjects as coronary atherosclerosis was present in a large proportion of the current cohort. Atherosclerosis may result in endothelial dysfunction and consequently impair myocardial perfusion even in the absence of severe stenosis. Thus, the

 https://doi.org/10.3348/kjr.2020.0249

current results cannot represent the normal MBF value in healthy subjects. Finally, other confounding factors, such as traditional risk factors of CAD, also contributed to the hyperemic effect after stress and consequently the range of MBF. Therefore, the results of the present study need to be validated by future studies with larger sample size to adjust the effect of the confounding factors.

In conclusion, global MBF value was found to be associated with the extent of change in HR after stress. Significantly higher global MBF was seen in subjects with HR increment of ≥ 20 bpm.

Conflicts of Interest

The authors have no potential conflicts of interest to disclose.

ORCID iDs

Lihua Yu
https://orcid.org/0000-0003-0586-3780
Xiaofeng Tao
https://orcid.org/0000-0003-1607-3522
Xu Dai
https://orcid.org/0000-0002-7487-6713
Ting Liu
https://orcid.org/0000-0002-0667-4044
Jiayin Zhang
https://orcid.org/0000-0001-7383-7571

REFERENCES

1. Bamberg F, Becker A, Schwarz F, Marcus RP, Greif M, von Ziegler F, et al. Detection of hemodynamically significant coronary artery stenosis: incremental diagnostic value of dynamic CT-based myocardial perfusion imaging. *Radiology* 2011;260:689-698
2. Bamberg F, Marcus RP, Becker A, Hildebrandt K, Bauner K, Schwarz F, et al. Dynamic myocardial CT perfusion imaging for evaluation of myocardial ischemia as determined by MR imaging. *JACC Cardiovasc Imaging* 2014;7:267-277
3. Coenen A, Rossi A, Lubbers MM, Kurata A, Kono AK, Chelu RG, et al. Integrating CT myocardial perfusion and CT-FFR in the work-up of coronary artery disease. *JACC Cardiovasc Imaging* 2017;10:760-770
4. Li Y, Yu M, Dai X, Lu Z, Shen C, Wang Y, et al. Detection of hemodynamically significant coronary stenosis: CT myocardial perfusion versus machine learning CT fractional flow reserve. *Radiology* 2019;293:305-314
5. Yu M, Chen X, Dai X, Pan J, Wang Y, Lu B, et al. The value of low-dose dynamic myocardial perfusion CT for accurate evaluation of microvascular obstruction in patients with acute myocardial infarction. *AJR Am J Roentgenol* 2019;213:798-806
6. Dai X, Yu M, Pan J, Lu Z, Shen C, Wanget Y, al. Image quality and diagnostic accuracy of coronary CT angiography derived from low-dose dynamic CT myocardial perfusion: a feasibility study with comparison to invasive coronary angiography. *Eur Radiol* 2019;29:4349-4356
7. Pan J, Yuan M, Yu M, Gao Y, Shen C, Wanget Y, al. Myocardial blood flow quantified by low-dose dynamic CT myocardial perfusion imaging is associated with peak troponin level and impaired left ventricle function in patients with ST-elevated myocardial infarction. *Korean J Radiol* 2019;20:709-718
8. Li Y, Yuan M, Yu M, Lu Z, Shen C, Wang Y, et al. Prevalence of decreased myocardial blood flow in symptomatic patients with patent coronary stents: insights from low-dose dynamic CT myocardial perfusion imaging. *Korean J Radiol* 2019;20:621-630
9. Kono AK, Coenen A, Lubbers M, Kurata A, Rossi A, Dharampal A, et al. Relative myocardial blood flow by dynamic computed tomographic perfusion imaging predicts hemodynamic significance of coronary stenosis better than absolute blood flow. *Invest Radiol* 2014;49:801-807
10. Karamitsos TD, Ntusi NA, Francis JM, Holloway CJ, Myerson SG, Neubauer S. Feasibility and safety of high-dose adenosine perfusion cardiovascular magnetic resonance. *J Cardiovasc Magn Reson* 2010;12:66
11. Bamberg F, Klotz E, Flohr T, Becker A, Becker CR, Schmidt B, et al. Dynamic myocardial stress perfusion imaging using fast dual-source CT with alternating table positions: initial experience. *Eur Radiol* 2010;20:1168-1173
12. Rossi A, Merkus D, Klotz E, Mollet N, de Feyter PJ, Krestin GP. Stress myocardial perfusion: imaging with multidetector CT. *Radiology* 2014;270:25-46
13. Fujita M, Kitagawa K, Ito T, Shiraishi Y, Kurobe Y, Nagata M, et al. Dose reduction in dynamic CT stress myocardial perfusion imaging: comparison of 80-kV/370-mAs and 100-kV/300-mAs protocols. *Eur Radiol* 2014;24:748-755
14. Cerqueira MD, Weissman NJ, Dilsizian V, Jacobs AK, Kaul S, Laskey WK, et al. Standardized myocardial segmentation and nomenclature for tomographic imaging of the heart. A statement for healthcare professionals from the Cardiac Imaging Committee of the Council on Clinical Cardiology of the American Heart Association. *Circulation* 2002;105:539-542
15. Meinel FG, Wichmann JL, Schoepf UJ, Pugliese F, Ebersberger U, Lo GG, et al. Global quantification of left ventricular myocardial perfusion at dynamic CT imaging: prognostic value. *J Cardiovasc Comput Tomogr* 2017;11:16-24
16. Tan SK, Yeong CH, Ng KH, Abdul Aziz YF, Sun Z. Recent update on radiation dose assessment for the state-of-the-art coronary computed tomography angiography protocols. *PLoS One* 2016;11:e0161543
17. Rossi A, Wragg A, Klotz E, Pirro F, Moon JC, Nieman K, et

https://doi.org/10.3348/kjr.2020.0249

al. Dynamic computed tomography myocardial perfusion imaging: comparison of clinical analysis methods for the detection of vessel-specific ischemia. *Circ Cardiovasc Imaging* 2017;10:e005505
18. Rossi A, Dharampal A, Wragg A, Davies LC, van Geuns RJ, Anagnostopoulos C, et al. Diagnostic performance of hyperaemic myocardial blood flow index obtained by dynamic computed tomography: does it predict functionally significant coronary lesions? *Eur Heart J Cardiovasc Imaging* 2014;15:85-94
19. Greif M, von Ziegler F, Bamberg F, Tittus J, Schwarz F, D'Anastasi M, et al. CT stress perfusion imaging for detection of haemodynamically relevant coronary stenosis as defined by FFR. *Heart* 2013;99:1004-1011
20. Ho KT, Ong HY, Tan G, Yong QW. Dynamic CT myocardial perfusion measurements of resting and hyperaemic blood flow in low-risk subjects with 128-slice dual-source CT. *Eur Heart J Cardiovasc Imaging* 2015;16:300-306
21. Kim EY, Chung WJ, Sung YM, Byun SS, Park JH, Kim JH, et al. Normal range and regional heterogeneity of myocardial perfusion in healthy human myocardium: assessment on dynamic perfusion CT using 128-slice dual-source CT. *Int J Cardiovasc Imaging* 2014;30 Suppl 1:33-40
22. van Assen M, Pelgrim GJ, De Cecco CN, Stijnen JMA, Zaki BM, Oudkerk M, et al. Intermodel disagreement of myocardial blood flow estimation from dynamic CT perfusion imaging. *Eur J Radiol* 2019;110:175-180
23. Murthy VL, Bateman TM, Beanlands RS, Berman DS, Borges-Neto S, Chareonthaitawee P, et al. Clinical quantification of myocardial blood flow using PET: joint position paper of the SNMMI Cardiovascular Council and the ASNC. *J Nucl Med* 2018;59:273-293
24. Pontone G, Baggiano A, Andreini D, Guaricci AI, Guglielmo M, Muscogiuri G, et al. Stress computed tomography perfusion versus fractional flow reserve CT derived in suspected coronary artery disease: the PERFECTION study. *JACC Cardiovasc Imaging* 2019;12(8 pt 1):1487-1497

 https://doi.org/10.3348/kjr.2020.0249